Afghanistan Journal of Infectious Diseases
AJID
https://ajid.ghalib.edu.af/index.php/ajid

2025 Jan 3(1): 56-73

Numerical Analysis of Typhoid Fever Spread Using Runge-Kutta and Nonstandard Finite Difference Methods

*Zabihullah Movaheedi, Behzad Heravi

Department of Mathematics, Faculty of Science, University of Herat, Herat, Afghanistan

ARTICLE INFO

Type: Original Article
Received: 2024/08/22
Accepted: 2024/12/30

*Corresponding Author:
E-mail:
z.movaheedi2@gmail.com

To cite this article: Movaheedi Z, Heravi B. Numerical Analysis of Typhoid Fever Spread Using Runge-Kutta and Nonstandard Finite Difference Methods. Afghanistan Journal of Infectious Diseases. 2025 Jan 3(1): 56-73. https://doi.org/10.60141/ajid.68

ABSTRACT

Background: Typhoid fever, caused by *Salmonella typhi*, spreads through food or water contaminated with manure, posing significant individual and public health risks. This study analyzes typhoid fever dynamics using a mathematical model with susceptible, unprotected, infected, and recovered populations.
Methods: The next-generation matrix was employed to compute the threshold quantity, evaluating the existence and stability of equilibrium points. Two numerical schemes were developed: a conditionally stable fourth-order Runge–Kutta (RK-4) scheme and an unconditionally stable nonstandard finite difference (NSFD) scheme. The NSFD scheme was designed to ensure dynamic reliability by preserving the continuous model's key properties. Numerical simulations were conducted using MATLAB R2015b.
Results: The RK-4 scheme maintained reliability only for smaller step sizes and did not preserve all essential properties of the original model. In contrast, the NSFD scheme accurately captured the dynamics of the model, maintaining positivity, boundedness, and monotonicity of solutions. Stability analyses revealed that the NSFD scheme converges locally and globally, irrespective of step size, for both disease-free and endemic equilibrium points.
Conclusion: The NSFD scheme preserves all critical dynamic properties of the continuous model and demonstrates its effectiveness in predicting the spread of typhoid fever. This study highlights the NSFD scheme as a robust numerical tool for modeling infectious disease dynamics, offering accurate and reliable results in alignment with the theoretical model.

Keywords: Typhoid fever; Mathematical modeling; Equilibrium stability; Runge–Kutta scheme; Nonstandard finite difference scheme

Introduction

Typhoid fever is a serious infectious disease caused by the bacterium *Salmonella typhi*, a human-specific pathogen that primarily infects the intestines and bloodstream (1). It spreads through contaminated food and water, leading to systemic infections that can become life-threatening without prompt treatment (2). Despite advancements in sanitation, this disease remains a significant public health challenge, particularly in developing nations (2, 3). Common symptoms include headache, stomach pain, joint pain, muscle aches, loss of appetite, diarrhea, skin spots, and fever (4). Without treatment, typhoid fever can lead to severe complications, including internal bleeding and abdominal infections due to the release of bacterial toxins (5). Diagnosis involves blood or stool tests to detect *S. Typhi* (6). Preventive measures include antibiotics, vaccinations, proper sanitation practices, and access to clean water (7). Vaccination remains a critical component of typhoid prevention,

with current options including the injectable Vi polysaccharide vaccine, which is approximately 65% effective, and the oral Ty21a vaccine (8, 9). The first typhoid vaccine was introduced over a century ago (10), and newer formulations continue to be developed to improve efficacy and accessibility.

Although preventive measures have reduced the burden of typhoid fever, the disease continues to pose a significant risk in many parts of the world, especially where access to clean water and sanitation is limited. Understanding the spread and control of typhoid is crucial for developing effective public health strategies. In this context, mathematical models play an essential role by providing a framework for analyzing the transmission dynamics of typhoid fever. These models allow researchers and policymakers to simulate different intervention strategies, predict outbreak scenarios, and assess the potential impact of vaccination, sanitation, and other control measures (11).

Over the years, various mathematical models have been developed to capture the dynamics of typhoid transmission, each offering valuable insights into disease control. For instance, recent models (12, 13) have incorporated vaccination and sanitation measures to evaluate the effectiveness of different strategies. Others focus on understanding the indirect protection conferred by vaccines and how this impacts overall transmission (14, 15). Such models are vital for predicting outbreak potential, designing control programs, and guiding public health interventions.

Building on these previous efforts, this study aimed to develop a mathematical model that captures the dynamics of typhoid fever among susceptible, unprotected, infected, and recovered populations. The focus is on evaluating two numerical schemes: the widely used RK-4 and NSFD scheme. Although the RK-4 method is a common choice due to its simplicity and high accuracy for solving ordinary differential equations, it has certain limitations when applied to models of disease dynamics. Specifically, RK-4 may fail to preserve essential qualitative properties of the underlying model, such as the non-negativity of solutions, which is critical since population variables (e.g., number of infected individuals) must remain positive. Additionally, RK-4 can struggle to maintain the boundedness and monotonicity of solutions, particularly when larger step sizes are used, potentially leading to inaccurate predictions of disease behavior. The NSFD scheme, on the other hand, is designed to overcome these limitations by ensuring that important dynamical properties—such as positivity, boundedness, and stability—are preserved, even with larger step sizes, thus improving the reliability of numerical simulations in capturing the true behavior of the model (16).

The objectives of this study were: 1) evaluate the existence and stability of disease-free and endemic equilibrium points using mathematical and numerical methods; 2) compare the dynamic reliability of the RK-4 and NSFD schemes; and 3) validate the NSFD scheme's effectiveness in accurately capturing the dynamics of typhoid fever regardless of step size. By addressing these questions, the study aims to determine which numerical method best preserves the essential features of the original model, ensuring accurate and reliable predictions of disease dynamics.

The introduction of qualitative dynamical numerical schemes, particularly the NSFD scheme pioneered by R. Mickens, represents a significant advancement in mathematical modeling. These schemes maintain critical features of the original continuous systems, aligning more closely with theoretical expectations than traditional methods like RK-4 (17). The NSFD scheme provides a more accurate and reliable representation of the original typhoid fever model, making it a valuable tool for predicting and managing disease spread.

Mathematical model and parameter explanations

In this study, we discuss and analyze a deterministic model for the compass dynamics of typhoid disease. The model assumes that the total population $N(t)$ is divided into four categories: susceptible (S), exposed (E), infected (I), and recovered (R), such that $N(t) = S(t) + E(t) + I(t) + R(t)$. The progression follows the sequence $S \to E \to I \to R$. Following is the SEIR disease system, a system of nonlinear ordinary differential equations (17):

$$\frac{dS}{dt} = \varphi + \sigma R - \alpha SI - \psi S$$

$$\frac{dE}{dt} = \alpha SI - \tau E - \psi E$$

$$\frac{dI}{dt} = \tau E - \theta I - \psi I$$

$$\frac{dR}{dt} = \theta I - \sigma R - \psi R. \quad \text{(eq. 1)}$$

Where the susceptible population increases through births or recruitment (φ) and from recovered individuals who lose immunity(σR), while it decreases due to disease interactions with the infected population (αSI) or natural death(ψS). The exposed population, infected but not yet infectious, grows through interactions with the infected (αSI) and diminishes as individuals either become infectious(τE) or die (ψE). The infected population rises as exposed individuals become infectious (τE) but shrinks due to recovery(θI), natural death(ψI), or death from illness(δI). Finally, the recovered population grows through recovery (θI), but individuals can lose immunity and return to the susceptible group (σR) or die naturally (ψR).

Figure 1 is the SEIR model diagram which is illustrates the flow of individuals between compartments. Arrows indicate transitions between the different stages of the disease. Individuals move from susceptible to exposed upon interaction with the infected population, from exposed to infect when symptoms develop, and from infected to recover upon recovery. Some recovered individuals lose immunity and return to the susceptible class. Natural death occurs in each compartment. This flow represents the dynamics of typhoid fever transmission, incorporating recruitment, natural death, recovery, and immunity loss.

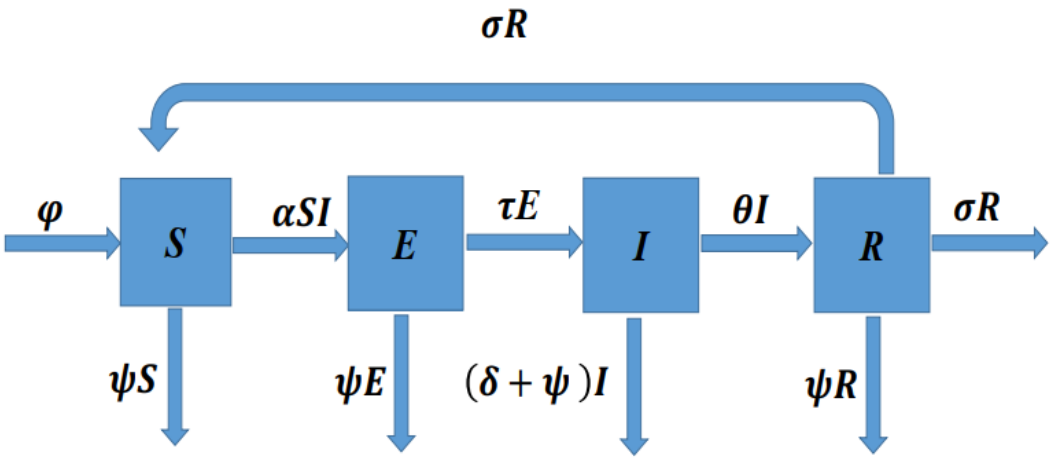

Figure 1: Detailed description of the epidemic model for typhoid fever transmission.

Parameters

The parameters used in Model (eq. 1) are detailed below (Table 1).

Justification for Model Structure

The SEIR structure is chosen to capture the sequential nature of typhoid transmission: individuals move from being susceptible to exposed (where they are infected but not yet symptomatic), then to the infectious stage, and finally to recovery. This model assumes:

- ✓ Permanent immunity is not conferred, hence the inclusion of a compartment for individuals losing immunity and re-entering the susceptible class.
- ✓ Birth and natural death occur continuously in the population, balancing population growth and decay.
- ✓ Disease-induced death affects the infected population, representing severe cases.

These assumptions align with the biological progression of typhoid and allow the model to account for factors such as immunity loss and the disease's long incubation period.

Table 1: Model key parameters with descriptions and sources

Parameter	*Description*	*Value*	*Reference*
ψ	The rate at which individuals die from natural causes.	0.02	(29)
δ	The rate at which infected individuals die due to the illness.	0.625	(30)
φ	The rate of birth or entry of new individuals into the population.	0.75	(19)
α	The rate at which susceptible individuals become exposed due to interaction with infected individuals.	0.925	(31)
τ	The rate at which exposed individuals become infectious.	0.0125	(28)
θ	The rate at which infected individuals recover and move to the recovered compartment.	0.1503	(27)
σ	The rate at which recovered individuals lose temporary immunity and become susceptible again.	0.125	(11)

All the parameters $\psi, \delta, \varphi, \alpha, \tau, \theta$, and σ are positive real constants.

Model Limitations

This model assumes homogeneous mixing, meaning that all individuals have an equal probability of contacting others. This may not accurately represent real-world interactions where population structure and social behavior can influence transmission. Additionally, the model assumes that recovered individuals have temporary immunity, but it does not account for vaccination or long-term immunity. The effects of environmental factors, such as water sanitation and public health interventions, are also not explicitly included in this framework. Future work could explore incorporating these factors for a more detailed analysis of typhoid transmission.

Equilibrium points and basic reproductive number

In this section, we derive the equilibrium points for the model (eq. 1) and the basic reproductive number R_0, providing the necessary intermediate steps and biological interpretations.

Equilibrium points

We consider the system of equations (eq. 1) and find two non-negative equilibria: the

disease-free equilibrium (DFE) and the disease-endemic equilibrium (DEE).

1. At the disease-free equilibrium (DFE), there are no exposed (E), infectious (I), or recovered (R) individuals in the population, meaning the entire population is susceptible. The DFE is given by:

$$E^0 = (S^0, E^0, I^0, R^0) = \left(\frac{\varphi}{\psi}, 0,0,0\right).$$

Here, $S^0 = \varphi/\psi$ represents the susceptible population, determined by the birth rate φ and the death rate ψ. The other compartments E^0, I^0, and R^0 are all zero since there is no disease present in the population at equilibrium.

2. The disease-endemic equilibrium (DEE) occurs when the disease persists in the population, and all compartments have non-zero values. The endemic equilibrium $E^* = (S^*, E^*, I^*, R^*)$ is given by:

$$S^* = \frac{(\tau+\psi)(\theta+\delta+\psi)}{\alpha\tau}, E^* = \frac{(\theta+\delta+\psi)(\sigma+\psi)\left(\varphi\tau\alpha - \psi(\tau+\psi)(\theta+\delta+\psi)\right)}{\alpha\tau(\sigma+\psi)(\tau+\psi)(\theta+\delta+\psi) - \theta\tau\sigma}$$

$$I^* = \frac{(\sigma+\psi)}{\alpha}\left(\frac{\varphi\tau\alpha - \psi(\tau+\psi)(\theta+\delta+\psi)}{(\sigma+\psi)(\tau+\psi)(\theta+\delta+\psi) - \theta\tau\sigma}\right), R^* = \frac{1}{\alpha}\frac{(\theta\varphi\tau\alpha - \theta\psi((\tau+\psi)(\theta+\delta+\psi))}{\left((\sigma+\psi)(\tau+\psi)(\theta+\delta+\psi) - \theta\tau\sigma\right)}$$

Basic Reproductive Number (R_0)

The basic reproductive number (R_0) is a crucial epidemiological metric that represents the average number of secondary infections caused by one infectious individual in a fully susceptible population. It helps to determine whether a disease will spread or die out in a population. To find the reproductive number, we use the next generation matrix concept from the authors in (18). For the model of typhoid fever disease (eq. 1), we can easily get

$$R_0 = \frac{\alpha\varphi\tau}{\psi(\tau+\psi)(\theta+\delta+\psi)}$$

Implications of Equilibria for Disease Dynamics

• Disease-Free Equilibrium (DFE): At $R_0 < 1$, the disease-free equilibrium is stable, meaning the disease will eventually be eradicated from the population. This scenario corresponds to effective control measures, such as vaccination or treatment that reduce R_0 below 1.

• Disease-Endemic Equilibrium (DEE): At $R_0 > 1$, the disease-endemic equilibrium is stable, indicating that the disease will persist in the population at a constant level. This suggests that interventions are insufficient to completely eliminate the disease, and it will continue to circulate unless more effective control measures are implemented.

In the next two sections, we will compare the NSFD method with the well-known RK-4 method. We are mostly focused on the NSFD plan, so we will talk a lot about its benefits and how it is used. This text talks about common issues with these systems, such as balance points, stability, and positivity, especially regarding how increasing the time step affects them. Moreover, this text talks about the important property of unconditional convergence for any step size, not covered in previous writings.

The RK-4 Method

The RK-4 method is a popular way to solve systems of ordinary differential equations (18). For most problems, we use the RK-4 method unless told to use something different. Let S be M_1, E be N_1, I be P_1, and R be Q_1. Then, the RK-4 method can be shown for system (eq. 1) as described below.

Step -1

$$M_1 = h[\varphi + \sigma R_n - \alpha S_n I_n - \psi S_n]$$
$$N_1 = h[\alpha S_n I_n - \tau E_n - \psi E_n]$$
$$P_1 = h[\tau E_n - \theta I_n - \delta I_n - \psi I_n]$$
$$Q_1 = h[\theta I_n - \sigma R_n - \psi R_n]$$

Step-2

$$M_2 = h\left[\varphi + \sigma\left(R_n + \frac{Q_1}{2}\right) - \alpha\left(S_n + \frac{M_1}{2}\right)\left(I_n + \frac{P_1}{2}\right) - \psi\left(S_n + \frac{M_1}{2}\right)\right]$$
$$N_2 = h\left[\alpha\left(S_n + \frac{M_1}{2}\right)\left(I_n + \frac{P_1}{2}\right) - \tau\left(E_n + \frac{N_1}{2}\right) - \psi\left(E_n + \frac{N_1}{2}\right)\right]$$
$$P_2 = h\left[\tau\left(E_n + \frac{N_1}{2}\right) - \theta\left(I_n + \frac{P_1}{2}\right) - \delta\left(I_n + \frac{P_1}{2}\right) - \psi\left(I_n + \frac{P_1}{2}\right)\right]$$
$$Q_2 = h\left[\theta\left(I_n + \frac{P_1}{2}\right) - \sigma\left(R_n + \frac{Q_1}{2}\right) - \psi\left(R_n + \frac{Q_1}{2}\right)\right]$$

Step-3

$$M_3 = h\left[\varphi + \sigma\left(R_n + \frac{Q_2}{2}\right) - \alpha\left(S_n + \frac{M_2}{2}\right)\left(I_n + \frac{P_2}{2}\right) - \psi\left(S_n + \frac{M_2}{2}\right)\right]$$
$$N_3 = h\left[\alpha\left(S_n + \frac{M_2}{2}\right)\left(I_n + \frac{P_2}{2}\right) - \tau\left(E_n + \frac{N_2}{2}\right) - \psi\left(E_n + \frac{N_2}{2}\right)\right]$$
$$P_3 = h\left[\tau\left(E_n + \frac{N_2}{2}\right) - \theta\left(I_n + \frac{P_2}{2}\right) - \delta\left(I_n + \frac{P_2}{2}\right) - \psi\left(I_n + \frac{P_2}{2}\right)\right]$$
$$Q_3 = h\left[\theta\left(I_n + \frac{P_2}{2}\right) - \sigma\left(R_n + \frac{Q_2}{2}\right) - \psi\left(R_n + \frac{Q_2}{2}\right)\right]$$

Step-4

$$M_4 = h[\varphi + \sigma(R_n + Q_3) - \alpha(S_n + M_3)(I_n + P_3) - \psi(S_n + M_3)]$$
$$N_4 = h[\alpha(S_n + M_3)(I_n + P_3) - \tau(E_n + N_3) - \psi(E_n + N_3)]$$
$$P_4 = h[\tau(E_n + N_3) - \theta(I_n + P_3) - \delta(I_n + P_3) - \psi(I_n + P_3)]$$
$$Q_4 = h[\theta(I_n + P_3) - \sigma(R_n + Q_3) - \psi(R_n + Q_3)]$$

Hence, the common system is

$$y_{n+1} = y_n + \Delta y$$
$$S_{n+1} = S_n + \frac{1}{6}\{M_1 + 2M_2 + 2M_3 + M_4\}$$
$$E_{n+1} = E_n + \frac{1}{6}\{N_1 + 2N_2 + 2N_3 + N_4\}$$
$$I_{n+1} = I_n + \frac{1}{6}\{P_1 + 2P_2 + 2P_3 + P_4\}$$
$$R_{n+1} = R_n + \frac{1}{6}\{Q_1 + 2Q_2 + 2Q_3 + Q_4\}$$

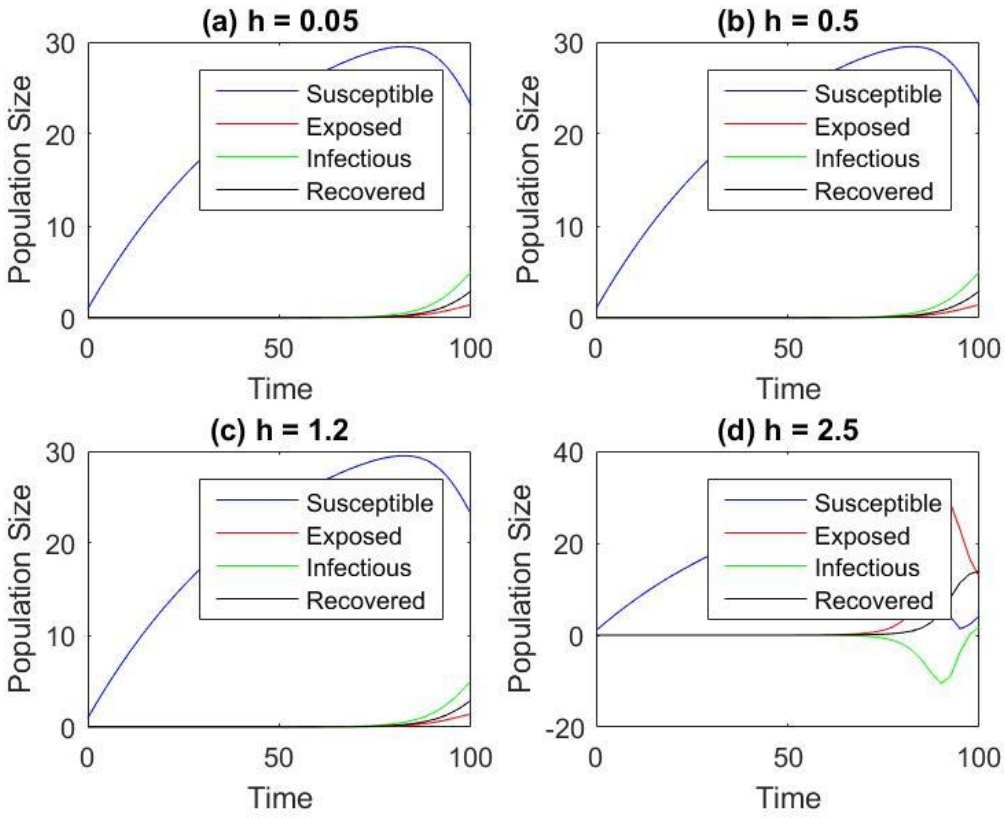

Figure 2: Numerical simulation of the SEIR model (eq. 1) via the RK-4 scheme with (a) h=0.05, (b) h= 0.5, (c) h=1.2, (d) h=2.5. The other parameters remain fixed as φ=0.75, α=0.0125, τ=0.925, ψ=0.02, θ=0.1503, δ=0.625, σ=0.125.

A picture showing the RK-4 method is displayed with various step sizes in the Figure 2. As "2 (a-d)" does not give me enough information. Figure 2 (a, b) shows that the RK-4 method gives good and steady results when using small step sizes. When we make the step size bigger, the stability of the balance point is lost for Model (eq. 1). Therefore, the RK-4 method won't work well with big step sizes.

The NSFD Scheme

In this part, we want to talk about how the NSFD plan works for Model (eq. 1). The NSFD scheme is a step-by-step method where we get closer to an answer by repeating the process several times (19). The NSFD scheme idea was introduced by Mickens (20). The NSFD method is a useful way to tackle issues in studying diseases, the environment, and groups of connected populations (21). In the following, we will demonstrate that no matter the size of the step (h), the discrete NSFD method keeps all the important behavior of the related continuous model (eq. 1).

Building the NSFD Plan

In model (eq. 1), we useS_n, E_n, I_n, and R_n to represent the calculated values of $S(t), E(t), I(t)$, and $R(t)$ at specific times $t = nh$, where n can be $0, 1, 2, 3$, and so on. Here, h is the time step, which should be a positive number or zero (22).

$$s_{n+1} - S_n = h(\varphi + \sigma R_n - \alpha S_{n+1} I_n - \psi S_{n+1})$$
$$E_{n+1} - E_n = h(\alpha S_{n+1} I_n - \tau E_{n+1} - \psi E_{n+1})$$
$$R_{n+1} - R_n = h(\theta I_{n+1} - \sigma R_{n+1} - \psi R_{n+1}).$$

The initial values of the discrete NSFD SEIR model (eq. 2) are all zero or positive, meaning S_0, E_0, I_0 and R_0 are greater than or equal to 0. You can find the clear version

of the discrete NSFD method (eq. 2) by getting it in this way:

$$S_{n+1} = \frac{S_n + h\varphi + h\alpha R_n}{1 + h(\alpha I_n + \psi)}$$
$$E_{n+1} = \frac{E_n + h\alpha S_{n+1} I_n}{1 + h\psi + h\tau} \qquad (eq.3)$$
$$R_{n+1} = \frac{R_n + h\theta I_{n+1}}{1 + h\sigma + h\psi}.$$

Next, we explain when the DFE and DEE points are stable or unstable for the discrete NSFD method. To reach this goal, we will first talk about how stable each of the balance points is.

Analyzing Local Stability for the Discrete NSFD Method

To show that the DFE and DEE points are locally stable (locally asymptotically steady LAS), we look at

$$S_{n+1} = \frac{S_n + h\varphi + h\alpha R_n}{1 + h(\alpha I_n + \psi)} = F_1$$
$$E_{n+1} = \frac{E_n + h\alpha S_{n+1} I_n}{1 + h(\psi + \tau)} = F_2 \qquad (eq.4)$$
$$R_{n+1} = \frac{R_n + h\theta I_{n+1}}{1 + h(\sigma + \psi)} = F_4.$$

To prove that the DFE and DEE points are LAS, we apply the Schur-Cohn rule (22) mentioned in Lemma 1.

Explanation

The Schur-Cohn rule is used to ensure that the equilibrium points are stable. It applies to the discrete system and guarantees that all eigenvalues of the Jacobian matrix have magnitudes less than 1. This ensures local asymptotic stability.

Lemma 1: The answers to the equation $\lambda^2 - T\lambda + D = 0$ will be less than 1 for $(|\lambda_i| < 1, i = 1,2)$ if and only if certain conditions are met.

1. $D < 1$,
2. $1 + D + T > 0$,
3. $1 - T + D > 0$,

where D and T signify the determinant and follow of the Jacobian lattice, individually.

Theorem 1: In the event that $R_0 < 1$, at that point the DFE point E^0 of the NSFD conspire (eq. 3) is the LAS for all $h > 0$.

Proof: Let us consider the Jacobian matrix

$$J(S,E,I,R) = \begin{bmatrix} \frac{\partial F_1}{\partial S} & \frac{\partial F_1}{\partial E} & \frac{\partial F_1}{\partial I} & \frac{\partial F_1}{\partial R} \\ \frac{\partial F_2}{\partial S} & \frac{\partial F_2}{\partial E} & \frac{\partial F_2}{\partial I} & \frac{\partial F_2}{\partial R} \\ \frac{\partial F_3}{\partial S} & \frac{\partial F_3}{\partial E} & \frac{\partial F_3}{\partial I} & \frac{\partial F_3}{\partial R} \\ \frac{\partial F_4}{\partial S} & \frac{\partial F_4}{\partial E} & \frac{\partial F_4}{\partial E} & \frac{\partial F_4}{\partial R} \end{bmatrix}. \qquad (eq.5)$$

As the below, we calculate all partial derivatives in (eq. 5):

$$\frac{\partial F_1}{\partial S} = \frac{1}{1 + h(\alpha I_n + \psi)}, \frac{\partial F_1}{\partial E} = 0, \frac{\partial F_1}{\partial I} = \frac{-h\alpha(S_n + h\varphi + h\alpha R_{n+1})}{\left(1 + h(\alpha I_n + \psi)\right)^2}, \frac{\partial F_1}{\partial R}$$
$$= \frac{h\alpha}{1 + h(\alpha I_n + \psi)}, \frac{\partial F_2}{\partial S} = \frac{h\alpha I_n}{1 + h\psi + h\tau}, \frac{\partial F_2}{\partial E} =$$

$$\frac{1}{1+h(\psi+\tau)}, \frac{\partial F_2}{\partial I} = \frac{h\alpha S_{n+1}}{1+h(\psi+\tau)}, \frac{\partial F_2}{\partial R} = 0, \frac{\partial F_3}{\partial S} = 0, \frac{\partial F_3}{\partial E} = \frac{h\tau}{1+h(\theta+\delta+\psi)}, \frac{\partial F_3}{\partial I} = \frac{1}{1+h(\theta+\delta+\psi)}, \frac{\partial F_3}{\partial R} = 0, \frac{\partial F_4}{\partial S} = 0, \frac{\partial F_4}{\partial E} = 0, \frac{\partial F_4}{\partial I} = \frac{h\theta}{1+h(\sigma+\psi)}, \frac{\partial F_4}{\partial R} = \frac{1}{1+h(\sigma+\psi)}.$$

Putting the values of all partial derivatives in (eq. 5), we get

$$J = \begin{bmatrix} \frac{1}{1+h(\alpha I_n+\psi)} & 0 & \frac{-h\alpha(S_n+h\varphi+h\alpha R_{n+1})}{(1+h(\alpha I_n+\psi))^2} & \frac{h\alpha}{1+h(\alpha I_n+\psi)} \\ \frac{h\alpha I_n}{1+h\psi+h\tau} & \frac{1}{1+h(\psi+\tau)} & \frac{h\alpha S_{n+1}}{1+h(\psi+\tau)} & 0 \\ 0 & \frac{h\tau}{1+h(\theta+\delta+\psi)} & \frac{1}{1+h(\theta+\delta+\psi)} & 0 \\ 0 & 0 & \frac{h\theta}{1+h(\sigma+\psi)} & \frac{1}{1+h(\sigma+\psi)} \end{bmatrix}.$$

At DFE point $E^0 = \left(\frac{\varphi}{\psi}, 0,0,0\right)$, the Jacobian changes to:

$$J(E^0) = \begin{bmatrix} \frac{1}{1+h\psi} & 0 & \frac{-h\alpha\left(\frac{\varphi}{\psi}+h\varphi\right)}{(1+h\psi)^2} & \frac{h\alpha}{1+h\psi} \\ 0 & \frac{1}{1+h(\psi+\tau)} & \frac{h\alpha\frac{\varphi}{\psi}}{1+h(\psi+\tau)} & 0 \\ 0 & \frac{h\tau}{1+h(\theta+\delta+\psi)} & \frac{1}{1+h(\theta+\delta+\psi)} & 0 \\ 0 & 0 & \frac{h\theta}{1+h(\sigma+\psi)} & \frac{1}{1+h(\sigma+\psi)} \end{bmatrix}.$$

To calculate the eigenvalues, we consider

$$\begin{vmatrix} \frac{1}{1+h\psi}-\lambda & 0 & \frac{-h\alpha\left(\frac{\varphi}{\psi}+h\varphi\right)}{(1+h\psi)^2} & \frac{h\alpha}{1+h\psi} \\ 0 & \frac{1}{1+h(\psi+\tau)}-\lambda & \frac{h\alpha\frac{\varphi}{\psi}}{1+h(\psi+\tau)} & 0 \\ 0 & \frac{h\tau}{1+h(\theta+\delta+\psi)} & \frac{1}{1+h(\theta+\delta+\psi)}-\lambda & 0 \\ 0 & 0 & \frac{h\theta}{1+h(\sigma+\psi)} & \frac{1}{1+h(\sigma+\psi)}-\lambda \end{vmatrix} = 0.$$

This equation can be written as:

$$\left(\frac{1}{1+h\psi}-\lambda\right)\left(\frac{1}{1+h(\sigma+\psi)}-\lambda\right)\begin{vmatrix} \frac{1}{1+h(\psi+\tau)}-\lambda & \frac{h\alpha\frac{\varphi}{\psi}}{1+h(\psi+\tau)} \\ \frac{h\tau}{1+h(\theta+\delta+\psi)} & \frac{1}{1+h(\theta+\delta+\psi)}-\lambda \end{vmatrix} = 0. \text{ (eq. 6)}$$

Equation (eq. 6) yields $\lambda_1 = \frac{1}{1+h\psi} < 1$ and $\lambda_2 = \frac{1}{1+h(\sigma+\psi)} < 1$. To calculate the other two eigenvalues, we solve the following equation

$$\begin{vmatrix} \frac{1}{1+h(\psi+\tau)}-\lambda & \frac{h\alpha\frac{\varphi}{\psi}}{1+h(\psi+\tau)} \\ \frac{h\tau}{1+h(\theta+\delta+\psi)} & \frac{1}{1+h(\theta+\delta+\psi)}-\lambda \end{vmatrix} = 0.$$

The below quadratic equation is obtained from solving the above equation:

$$\lambda^2 - \lambda\left(\frac{1}{1+h(\psi+\tau)}+\frac{1}{1+h(\theta+\delta+\psi)}\right)+\frac{1}{(1+h(\theta+\delta+\psi))(1+h(\psi+\tau))}-\frac{h\alpha\varphi}{\psi(1+h(\psi+\tau))(1+h(\theta+\delta+\psi))} = 0. \text{ (eq. 7)}$$

Comparing (7) with $\lambda^2 - T\lambda + D = 0$, we obtain $T = \frac{1}{1+h(\psi+\tau)} + \frac{1}{1+h(\theta+\delta+\psi)}$ and $D = \frac{1}{(1+h(\theta+\delta+\psi))(1+h(\psi+\tau))} - \frac{h\alpha\varphi}{\psi(1+h(\psi+\tau))(1+h(\theta+\delta+\psi))}$. If $R_0 < 1$, i.e., $\alpha\varphi\tau < \psi(\tau+\psi)(\theta+\delta+\psi)$, then all three conditions of Lemma 1 are satisfied.

1. $D = \frac{1}{(1+h(\theta+\delta+\psi)(1+h(\psi+\tau))} + \frac{h\alpha\varphi}{\psi(1+h(\psi+\tau))(1+h(\theta+\delta+\psi))} < 1.$
2. $1 + T + D = 1 + \frac{1}{1+h(\psi+\tau)} + \frac{1}{1+h(\theta+\delta+\psi)} + \frac{1}{(1+h(\theta+\delta+\psi)(1+h(\psi+\tau))} - \frac{h\alpha\varphi}{\psi(1+h(\psi+\tau))(1+h(\theta+\delta+\psi))}. > 0.$
3. $1 - T + D = 1 - \frac{1}{1+h(\psi+\tau)} - \frac{1}{1+h(\theta+\delta+\psi)} + \frac{1}{(1+h(\theta+\delta+\psi)(1+h(\psi+\tau))} - \frac{h\alpha\varphi}{\psi(1+h(\psi+\tau))(1+h(\theta+\delta+\psi))} > 0.$

Therefore, all the requirements for the Schur-Cohn rule mentioned in Lemma 1 are met whenever R_0 is less than 1. The DFE point E^0 of the discrete NSFD scheme (eq. 3) is the LAS if R_0 is less than 1.

Explanation

The Schur-Cohn rule is used to ensure that the equilibrium points are stable. It applies to the discrete system and guarantees that all eigenvalues of the Jacobian matrix have magnitudes less than 1. This ensures local asymptotic stability.

When a disease is common in a community, it will always be present among the people there. In the next theorem, we use the Routh-Hurwitz rule (23) to show that the DEE point E* is LAS.

Theorem 2: If R_0 is greater than 1, then the point E^* in the NSFD model (eq. 3) is the LAS for any positive value of h.

Proof: Let's look at the Jacobian matrix.

$$J(S,E,I,R) = \begin{bmatrix} \frac{\partial F_1}{\partial S} & \frac{\partial F_1}{\partial E} & \frac{\partial F_1}{\partial I} & \frac{\partial F_1}{\partial R} \\ \frac{\partial F_2}{\partial S} & \frac{\partial F_2}{\partial E} & \frac{\partial F_2}{\partial I} & \frac{\partial F_2}{\partial R} \\ \frac{\partial F_3}{\partial S} & \frac{\partial F_3}{\partial E} & \frac{\partial F_3}{\partial I} & \frac{\partial F_3}{\partial R} \\ \frac{\partial F_4}{\partial S} & \frac{\partial F_4}{\partial E} & \frac{\partial F_4}{\partial E} & \frac{\partial F_4}{\partial R} \end{bmatrix}. \quad \text{(eq. 8)}$$

By applying all the partial derivatives from Theorem 1 with (eq. 8), we get

$$J = \begin{bmatrix} \frac{1}{1+h(\alpha I_n+\psi)} & 0 & \frac{-h\alpha(S_n+h\varphi+h\alpha R_{n+1})}{(1+h(\alpha I_n+\psi))^2} & \frac{h\alpha}{1+h(\alpha I_n+\psi)} \\ \frac{h\alpha I_n}{1+h(\psi+\tau)} & \frac{1}{1+h(\psi+\tau)} & \frac{h\alpha S_{n+1}}{1+h(\psi+\tau)} & 0 \\ 0 & \frac{h\tau}{1+h(\theta+\delta+\psi)} & \frac{1}{1+h(\theta+\delta+\psi)} & 0 \\ 0 & 0 & \frac{h\theta}{1+h(\sigma+\psi)} & \frac{1}{1+h(\sigma+\psi)} \end{bmatrix}.$$

By putting the DEE point E^*, we get

$$J(E^*) = \begin{bmatrix} \frac{1}{1+h(\alpha I^*{}_{n}+\psi)} & 0 & \frac{-h\alpha(S^*{}_{n}+h\varphi+h\alpha R^*{}_{n+1})}{\left(1+h(\alpha I^*{}_{n}+\psi)\right)^2} & \frac{h\alpha}{1+h(\alpha I^*{}_{n}+\psi)} \\ \frac{h\alpha I^*{}_{n}}{1+h\psi+h\tau} & \frac{1}{1+h(\psi+\tau)} & \frac{h\alpha S^*{}_{n+1}}{1+h(\psi+\tau)} & 0 \\ 0 & \frac{h\tau}{1+h(\theta+\delta+\psi)} & \frac{1}{1+h(\theta+\delta+\psi)} & 0 \\ 0 & 0 & \frac{h\theta}{1+h(\sigma+\psi)} & \frac{1}{1+h(\sigma+\psi)} \end{bmatrix}.$$

Now we calculate the eigenvalues:

$$\begin{vmatrix} \frac{1}{1+h(\alpha I^*{}_{n}+\psi)}-\lambda & 0 & \frac{-h\alpha(S^*+h\varphi+h\alpha R^*{}_{n+1})}{\left(1+h(\alpha I^*{}_{n}+\psi)\right)^2} & \frac{h\alpha}{1+h(\alpha I^*{}_{n}+\psi)} \\ \frac{h\alpha I^*{}_{n}}{1+h\psi+h\tau} & \frac{1}{1+h(\psi+\tau)}-\lambda & \frac{h\alpha S^*{}_{n+1}}{1+h(\psi+\tau)} & 0 \\ 0 & \frac{h\tau}{1+h(\theta+\delta+\psi)} & \frac{1}{1+h(\theta+\delta+\psi)}-\lambda & 0 \\ 0 & 0 & \frac{h\theta}{1+h(\sigma+\psi)} & \frac{1}{1+h(\sigma+\psi)}-\lambda \end{vmatrix} = 0.$$

The characteristic equation for the equation mentioned above is

$$\lambda^4 + P_1\lambda^3 + P_2\lambda^2 + P_3\lambda + P_4 = 0, \qquad \text{(eq. 9)}$$

where

$$P_1 = \frac{1}{1+h(\alpha I^*{}_{n}+\psi)} + \frac{1}{1+h(\psi+\tau)} + \frac{1}{1+h(\theta+\delta+\psi)} + \frac{1}{1+h(\sigma+\psi)} > 0$$

$$P_2 = \frac{1}{(1+h(\theta+\delta+\psi))(1+h(\tau+\psi))} - \frac{h^2\tau\alpha S^*_{n+1}}{(1+h(\tau+\psi))(1+h(\theta+\delta+\psi))} - \left(\frac{1}{1+h(\alpha I^*{}_{n}+\psi)} + \frac{1}{1+h(\sigma+\psi)}\right)\left(\frac{1}{(1+h(\theta+\delta+\psi))(1+h(\tau+\psi))}\right) + \frac{1}{(1+h(\alpha I^*{}_{n}+\psi))(1+h(\sigma+\psi))} > 0$$

$$P_3 = \frac{1}{(1+h(\alpha l^*{}_{n}+\psi))} + \frac{1}{(1+h(\sigma+\psi))(1+h(\tau+\psi))(1+h(\theta+\delta+\psi)} + \frac{h^2\tau\alpha S^*_{n+1}}{(1+h(\alpha l^*{}_{n}+\psi))(1+h(\sigma+\psi))(1+h(\tau+\psi))(1+h(\theta+\delta+\psi)} + \frac{h^2\tau\alpha}{(1+h(\alpha l^*{}_{n}+\psi))(1+h(\alpha l^*{}_{n}+\psi)^2} + \frac{1}{(1+h(\alpha l^*{}_{n}+\psi))(1+h(\sigma+\psi))(1+h(\tau+\psi))(1+h(\theta+\delta+\psi)} > 0,$$

$$P_4 = \frac{h^2\tau\alpha(S^*{}_{n}+h\varphi+h\alpha R^*{}_{n})}{\left(1+h(\alpha l^*{}_{n}+\psi)(1+h(\alpha l^*{}_{n}+\psi)\right)^2(1+h(\sigma+\psi))} + \frac{h^3\tau\alpha\theta}{(1+h(\sigma+\psi))(1+h(\alpha l^*{}_{n}+\psi))(1+h(\alpha l^*{}_{n}+\psi))} + \frac{1}{(1+h(\alpha l^*{}_{n}+\psi))(1+h(\sigma+\psi))(1+h(\tau+\psi))(1+h(\theta+\delta+\psi))}.$$

Using the information given above, if R_0 is greater than 1, then.

$$M_1 = P_1 > 0$$

$$M_2 = P_1P_2 - P_3 > 0$$

$$M_3 = \begin{vmatrix} P_1 & P_3 & 0 \\ 1 & P_2 & P_4 \\ 0 & P_1 & P_3 \end{vmatrix} = -P_3^2 + P_1P_2P_3 - P_1^2P_4 = P_3M_2 - P_1^2P_4 > 0$$

$$M_4 = P_4M_3 > 0.$$

Therefore, when we use the Routh–Hurwitz method, all the solutions to the characteristic equation need to have negative real parts. When R_0 is greater than 1, the DEE point E^* of the discrete NSFD scheme (eq. 3) is the LAS.

Analyzing Global Stability for the Discrete NSFD Method

Next, we will explain that R_0 is the equilibria value for stability. If R_0 is less than or equal to 1, then the point E^0 is globally asymptotically stable (GAS). If R_0 is greater than 1, then the point E^* becomes the GAS point. To talk about the global

stability of equilibria, we use the same standard that Vaz and colleagues used (24).

Theorem 3: If R_0 is less than or equal to 1, then the DFE point E^0 of the NSFD model (eq. 3) is globally asymptotically stable for all positive values of h.

Proof: Let η be a number greater than 0. Then, there is an integer n_0 such that for any n that is equal to or greater than n_0, $S_{n+1} < \frac{\varphi}{\psi} + \eta$. Let's look at the sequence $w(n)$ starting from n equals 0 and going to infinity.

$$w(n) = E_n + \frac{\omega}{C_3} I_n + \frac{\alpha}{C_2} R_n + h\alpha S_{n+1} I_n$$

where $C_2 = (\sigma + \psi)$ and $C_3 = (\theta + \delta + \psi)$. For $n \geq n_0$, we have

$$\begin{aligned} w(n+1) - w(n) &= E_{n+1} + \frac{\omega}{C_3} I_{n+1} + \frac{\alpha}{C_2} R_{n+1} + h\alpha S_{n+2} I_{n+1} - E_n - \frac{\omega}{C_3} I_n - \frac{\alpha}{C_2} R_n \\ &\quad - h\alpha S_{n+1} I_n \\ &= (E_{n+1} - E_n) + \frac{\omega}{C_3} I_{n+1} + \frac{\alpha}{C_2} R_{n+1} + h\alpha S_{n+2} I_{n+1} - \frac{\omega}{C_3} I_n - \frac{\alpha}{C_2} R_n - h\alpha S_{n+1} I_n \\ &= (E_{n+1} - E_n) + \frac{\omega}{c_3} (I_{n+1} - I_n) + \frac{\alpha}{c_2} (R_{n+1} - R_n) + h\alpha S_{n+2} I_{n+1} - h\alpha S_{n+1} I_n \end{aligned}$$

Using the NSFD model (eq. 3), we get

$$\begin{aligned} &= h(\alpha S_{n+1} I_n - (\tau + \psi) E_{n+1}) + \frac{\omega}{c_3} h(\tau E_{n+1} - (\theta + \delta + \psi) I_{n+1}) + \frac{\alpha}{c_2} h(\theta I_{n+1} - \\ &\quad (\sigma + \psi) R_{n+1}) + h\alpha S_{n+2} I_{n+1} - h\alpha S_{n+1} I_n. \end{aligned}$$

Let $C_1 = (\tau + \psi)$; So, it turns into this:

$$\begin{aligned} &= h\left(\alpha S_{n+2} I_n + \frac{\omega}{C_3} (\tau E_{n+1} - (\theta + \delta + \psi) I_{n+1}) + \frac{\alpha}{c_2} (\theta I_{n+1} - (\sigma + \psi) R_{n+1}) - \right. \\ &\quad \left. C_1 E_{n+1})\right) \\ &= h\left(\alpha S_{n+2} I_n + \left(\frac{\omega\tau}{C_3} - C_1\right) E_{n+1} + \frac{\alpha}{C_2} \theta I_{n+1} - \frac{\omega}{C_3} (\theta + \delta + \psi) I_{n+1} - (\sigma + \psi) R_{n+1}\right) \\ &= h\left(\alpha S_{n+2} I_n + (\omega\tau - C_1 C_3) \frac{E_{n+1}}{C_3} + \left(\frac{\alpha\theta}{c_2} - \frac{\omega}{c_3} (\theta + \delta + \psi)\right) I_{n+1} - (\sigma + \psi) R_{n+1}\right). \end{aligned}$$

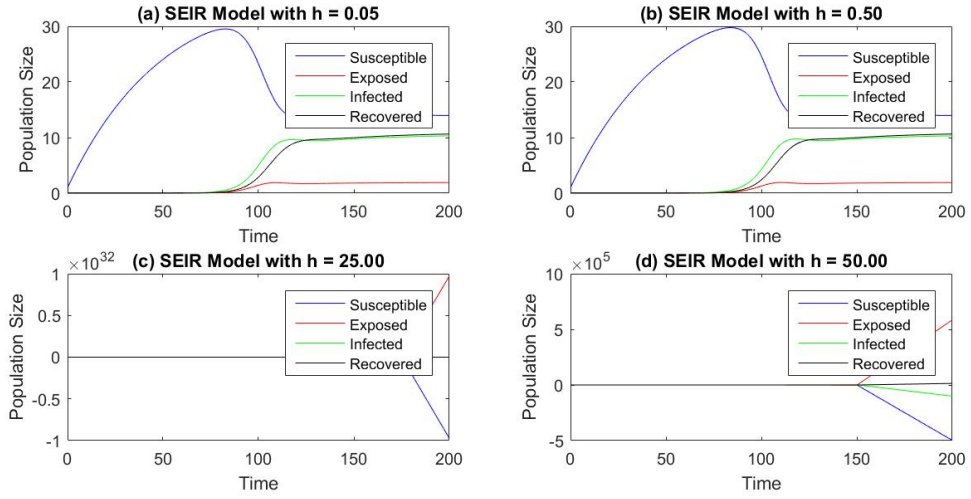

Figure 3: Numerical simulation of the SEIR model (1) via the NSFD scheme with (a) h=0.05, (b) h=0.5, (c)h=25, (d)h=50. The other parameters remain fixed as φ=0.75, α=0.0125, τ=0.925, ψ=0.02, θ=0.1503, δ=0.625, σ=0.125.

If we pick $C_1C_3 - \omega\tau = D$, the above expression changes to

$$= h\left(\left(\alpha S_{n+2}I_n - D\frac{E_{n+1}}{C_3}\right) - (\theta+\delta+\psi)I_{n+1} - (\sigma+\psi)R_{n+1}\right).$$

We can pick β to be a very small positive number so that

$$\alpha S_{n+2}I_n \le \beta(E_{n+1} + C_3I_{n+1} + C_2R_{n+1})$$
$$= \beta\left(E_{n+1} + C_3\frac{\tau}{C_3}E_{n+1} + C_2\frac{E_{n+1}}{C_2C_3}\right).$$

Therefore, we obtain

$$w(n+1) - w(n) \le h\left(\beta\left(E_{n+1} + \tau E_{n+1} + \frac{E_{n+1}}{C_3}\right) - D\frac{E_{n+1}}{C_3}\right)$$
$$\le \frac{hE_{n+1}}{C_3}\left(\beta + \beta\frac{\psi(\tau+\psi)(\theta+\delta+\psi)}{\alpha\varphi}\frac{\alpha\varphi\tau}{\psi(\tau+\psi)(\theta+\delta+\psi)} + \beta - D\right)$$
$$\le \frac{hE_{n+1}}{C_3}\left(\beta + \beta\frac{\psi(\tau+\psi)(\theta+\delta+\psi)}{\alpha\varphi}R_0 + \beta - D\right)$$
$$= \frac{hE_{n+1}}{C_3}\left(2\beta + \frac{\beta\psi(\tau+\psi)(\theta+\delta+\psi)}{\alpha\varphi}R_0 - D\right).$$

If $C = \frac{\psi(\tau+\psi)(\theta+\delta+\psi)}{\alpha\varphi}$; then, we receive

$$= \frac{hE_{n+1}}{C_3}(2\beta + C\beta R_0 - D)$$
$$= \frac{hE_{n+1}}{C_3}(\beta(2 + CR_0) - D).$$

Since β is a really small number and η is not exact, if R_0 is less than or equal to 1, we can conclude that $w(n+1) - w(n)$ is less than or equal to 0, and as n gets very large, I_n approaches 0 for any $n \ge 0$. The sequence $w(n)$ from $n = 0$ to infinity decreases steadily, and the limit of S_n as n approaches infinity is φ/ψ. So, when R_0 is less than or equal to 1, the DFE point E^0 is the GAS point (25, 26).

The numerical solution shown in the Figure 3 (a-d) also show that if R_0 is less than or equal to 1, then the results from the NSFD method (eq. 3) get closer to the DFE point regardless of the step size. The discrete NSFD method always gets closer to the solution for Model (eq. 1).

Theorem 4: If R_0 is greater than 1, then the DEE point E^* of the NSFD model (eq. 3) is GAS for any positive value of h.

Proof: Let's create a sequence $w(n)$ from $n = 0$ to infinity in the following way:

$w(n) = \frac{1}{hE^*}p\left(\frac{S_n}{S^*}\right) + \frac{1}{hS^*}p\left(\frac{E_n}{E^*}\right) + \frac{\omega I^*}{hC_3S^*E^*}p\left(\frac{I_n}{I^*}\right) + \frac{\alpha R^*}{hC_2S^*E^*}p\left(\frac{R_n}{R^*}\right)$,

as $p(x) = x - 1 - ln(x)$ for $x \in R^+, C_2 = \sigma + \psi$ and $C_3 = \theta + \delta + \psi$. It is obvious that $p(x) \ge 0$, and the equality stay true if $x = 1$. We can result

$$p\left(\frac{S_{n+1}}{S^*}\right)-p\left(\frac{S_n}{S^*}\right)=\frac{s_{n+1}-S_n}{S^*}-l\,n\left(\frac{s_{n+1}}{S_n}\right)$$
$$\leq\frac{(S_{n+1}-S^*)(S_{n+1}-S_n)}{S_{n+1}S^*}$$
$$=\frac{(S_{n+1}-S^*)}{S_{n+1}S^*}h(\varphi+\sigma R_n-\alpha S_{n+1}I_n-\psi S_{n+1})$$
$$=\frac{(S_{n+1}-S^*)}{S_{n+1}S^*}h(\alpha S^*I^*+\psi S^*-\sigma R_n-\alpha S_{n+1}I_n-\psi S_{n+1})$$
$$=h\big((S_{n+1}-S^*)(-\psi(S_{n+1}-S^*)-\alpha S_{n+1}I_n+\alpha S^*I^*-\sigma R_n)$$
$$=h\left((S_{n+1}-S^*)\left(-\psi(S_{n+1}-S^*)-\alpha\left(\frac{S_{n+1}I_n}{I^*S^*}-1\right)-\sigma R_n\right)\right.$$
$$=\frac{-\psi h(s_{n+1}-S^*)^2}{s_{n+1}S^*}-h\left(\alpha\left(1-\frac{S^*}{s_{n+1}}\right)\left(\frac{I_n}{I^*}\frac{s_{n+1}}{S^*}-1\right)-\sigma R_n\right).$$

In the same method,

$$p\left(\frac{E_{n+1}}{E^*}\right)-p\left(\frac{E_n}{E^*}\right)=\frac{E_{n+1}-E_n}{E^*}-l\,n\left(\frac{E_{n+1}}{E_n}\right)$$
$$\leq\frac{(E_{n+1}-E^*)(E_{n+1}-E_n)}{E_{n+1}E^*}$$
$$=\frac{(E_{n+1}-E^*)}{E_{n+1}E^*}(\alpha S_{n+1}I_n-\tau E_{n+1}-\psi E_{n+1})$$
$$=\frac{(E_{n+1}-E^*)}{E_{n+1}E^*}(\alpha S_{n+1}I_n-(\tau+\psi)E_{n+1}).$$

If $C_1=\tau+\psi$; then,

$$p\left(\frac{E_{n+1}}{E^*}\right)-p\left(\frac{E_n}{E^*}\right)\leq\frac{(E_{n+1}-E^*)}{E_{n+1}E^*}(\alpha S_{n+1}I_n-C_1E_{n+1})$$
$$=\frac{(E_{n+1}-E^*)}{E_{n+1}E^*}\left(\alpha S_{n+1}I_n-\frac{E_{n+1}\alpha S^*}{E^*}\right)$$
$$=\left(1-\frac{E^*}{E_{n+1}}\right)\frac{h\alpha S^*}{E^*}\left(\frac{I_n}{I^*}\frac{S_{n+1}}{S^*}-\frac{E_{n+1}}{E^*}\right).$$

and

$$p\left(\frac{I_{n+1}}{I^*}\right)-p\left(\frac{I_n}{I^*}\right)=\frac{I_{n+1}-I_n}{I^*}-l\,n\left(\frac{I_{n+1}}{I_n}\right)$$
$$\leq\frac{(I_{n+1}-I^*)(I_{n+1}-I_n)}{I_{n+1}I^*}$$
$$\leq\frac{(I_{n+1}-I^*)}{I_{n+1}I^*}(\tau E_{n+1}-(\theta+\delta+\psi)I_{n+1}$$
$$\leq\frac{(I_{n+1}-I^*)}{I_{n+1}I^*}(\tau E_{n+1}-C_3I_{n+1})$$
$$=C_3h\left(1-\frac{I^*}{I_{n+1}}\right)\left(\frac{E_{n+1}}{E^*}-\frac{I_{n+1}}{I^*}\right).$$

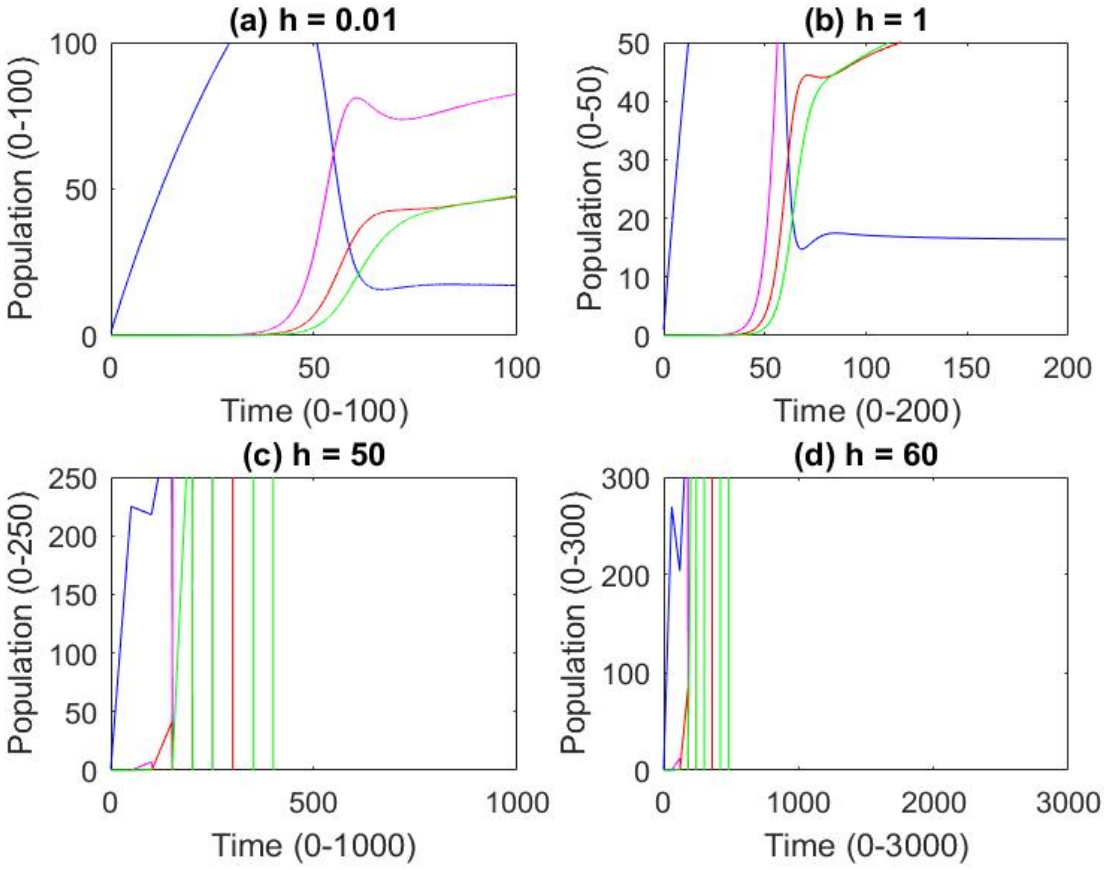

Figure 4: Numerical simulation of the SEIR model (1) via the NSFD scheme with (a)h=0.01, (b)h= 1, (c)h=50, (d)h=60. The other parameters remain fixed as φ=4.5, α=0.0125, τ=0.099925, ψ=0.02, θ=0.1503, δ=0.625, σ=0.125.

and

$$p\left(\frac{R_{n+1}}{R^*}\right) - p\left(\frac{R_n}{R^*}\right) = \frac{R_{n+1}-R_n}{R^*} - ln\left(\frac{R_{n+1}}{R_n}\right)$$
$$\leq \frac{(R_{n+1}-R^*)(R_{n+1}-R_n)}{R_{n+1}R^*}$$
$$\leq \frac{(R_{n+1}-R^*)}{R_{n+1}R^*}(\theta I_{n+1} - (\sigma+\psi)R_{n+1})$$
$$\leq \frac{(R_{n+1}-R^*)}{R_{n+1}R^*}(\theta I_{n+1} - C_2 R_{n+1})$$
$$= C_2 h\left(1 - \frac{R^*}{R_{n+1}}\right)\left(\frac{I_{n+1}}{I^*} - \frac{R_{n+1}}{R^*}\right).$$

The change in $w(n)$ meets the condition.

$$w(n+1)-w(n) = \frac{1}{hE^*}\left(p\left(\frac{S_{n+1}}{S^*}\right)-p\left(\frac{S_n}{S^*}\right)\right)+\frac{1}{hS^*}\left(p\left(\frac{E_{n+1}}{E^*}\right)-p\left(\frac{E_n}{E^*}\right)\right)$$
$$+\frac{\omega I^*}{hC_3S^*E^*}\left(p\left(\frac{I_{n+1}}{I^*}\right)-p\left(\frac{I_n}{I^*}\right)\right)+\frac{\alpha R^*}{hC_2S^*E^*}\left(p\left(\frac{R_{n+1}}{R^*}\right)-p\left(\frac{R_n}{R^*}\right)\right)$$
$$\leq\frac{-\alpha h(S_{n+1}-S^*)^2}{S_{n+1}S^*I^*}-\frac{\alpha}{E^*}\left(\frac{E^*}{E_{n+1}}\frac{I_n^*}{I^*}\frac{S_{n+1}}{S^*}-2-\frac{I_n}{I^*}+\frac{S^*}{S_{n+1}}+\frac{E_{n+1}}{E^*}\right)-\frac{\omega I^*}{S^*E^*}\left(\frac{E^*I_{n+1}}{E_{n+1}I^*}+\frac{I^*E_{n+1}}{I_{n+1}E^*}-\right.$$
$$\left.2\right)-\frac{\alpha R^*}{S^*E^*}\left(\frac{E^*R_{n+1}}{E_{n+1}R^*}+\frac{R^*E_{n+1}}{R_{n+1}E^*}-2\right)$$
$$\leq\frac{-\alpha h(S_{n+1}-S^*)^2}{S_{n+1}S^*I^*}-\frac{\alpha}{E^*}\left(p\left(\frac{S^*}{S_{n+1}}\right)+p\left(\frac{I_{n+1}}{I^*}\right)+p\left(\frac{E^*}{E_{n+1}}\frac{I_n}{I^*}\frac{S_{n+1}}{S^*}\right)-p\left(\frac{I_n}{I^*}\right)\right)-\frac{\omega\omega^*}{S^*E^*}$$
$$\left(p\left(\frac{E^*I_{n+1}}{E_{n+1}1^*}\right)+p\left(\frac{I^*E_{n+1}}{I_{n+1}E^*}\right)\right)-\frac{\alpha R^*}{S^*E^*}\left(p\left(\frac{E^*R_{n+1}}{E_{n+1}R^*}\right)+p\left(\frac{R^*E_{n+1}}{R_{n+1}E^*}\right)\right).$$

Therefore, for any number n that is 0 or greater, the sequence $w(n)$ from $n = 1$ to infinity decreases monotonically. Since $w(n)$ is always nonnegative and as n goes to infinity, the difference between $w(n+1)$ and $w(n)$ gets closer to 0, we can say that as n becomes very large, $S(n+1)$ approaches S^*, $E(n+1)$ approaches E^*, $I(n+1)$ approaches I^*, and $R(n+1)$ approaches R^*. This finishes the proof.

The numerical solution shown in the Figure 4 (a-d) also show that if R_0 is greater than 1, then the results from the NSFD method (3) will get close to the DEE point, no matter how big or small the step size is. The NSFD method is always convergent for the system given in (eq. 1).

Conclusion

This paper presents a model that looks at how typhoid fever spreads in a non-linear way. The spread of the disease mainly depends on how often people are in contact with sick individuals in the community. The RK-4 and NSFD methods are used to describe behaviors and properties, containing the local and global stability of the DFE and DEE points. The NSFD method fixes all disadvantages of the RK-4 method and provides accurate numerical solutions. Convergence shows that the method stays stable and keeps its positive features. The main advantages of this method have been shown theoretically and numerically. This approach works well, even when using large time intervals. This is a big benefit for implementing and computing. Moreover, the RK-4 method cannot accurately keep the main features of the original continuous model. This means it can give numerical solutions that are different from the original model's solutions. The NSFD scheme presents better outcomes for both society and the field of medical science.

Soon, we want to search other disease models that are similar to the one we are looking at. This will help us understand the risks to public health better. To show that it works well and is biologically sound, we create three different methods: Euler, RK-4, and NSFD, to examine various features of the model. Models of typhoid fever are particularly relevant in this regard.

Acknowledgments

The authors would like to thank Herat University, Herat, Afghanistan for its invaluable support and resources during this research.

Conflict of interest

The authors declare that there is no conflict of interests.

References

1. Maqsood A, Muhammad S, Farhan R, Mohsin K, Muhammad HR, Iqra J, Noore S, Akhlaaq W, Zahida Q. Typhoid Fever: Pakistan's Unique Challenges and Pragmatic Solutions. 2024. doi: 10.35787/jimdc.v13i1.1179.
2. Bhandari J, Thada PK, Hashmi MF, et al. Typhoid fever. [Updated 2024 Apr 19]. In: StatPearls [Internet]. Treasure Island (FL): StatPearls Publishing; 2024 Jan-. Available from: https://www.ncbi.nlm.nih.gov/books/NBK557513/.
3. Crump JA, Mintz ED. Global trends in typhoid and paratyphoid fever. Clin Infect Dis. 2019;68(Supplement_1).
4. Naushad M, Thobbi AN. A study of etiopathogenesis, clinical and laboratory profile evaluation of typhoid fever in paediatric age group in Bijapur. Int J Contemp Pediatr. 2023. doi: 10.18203/2349-3291.ijcp20231488.
5. Hatta M, Ratnawati V, Husni A. The immune response in typhoid fever: a review. J Clin Diagn Res. 2018;12(1).
6. Diwaker A, Tiwari A, Jain S, Rupali KA, Ram J, Singh S, Kishore D. Enteric fever and the diagnostic tools: defining the accuracy. Front Bacteriol. 2024 Jan 29;3:1332180.
7. Levine MM, Simon R. The gathering storm: is untreatable typhoid fever on the way? mBio. 2018;9(2).
8. Ochiai RL, Acosta CJ, Danovaro-Holliday MC, Baiqing D, Bhattacharya SK, Agtini MD, et al. A study of typhoid fever in five Asian countries: disease burden and implications for controls. Bull World Health Organ. 2019;86:260-8.
9. Abba A, Kassah-Laouar A, Amara A, Omari A. Modeling the transmission dynamics of typhoid fever with treatment and vaccination. J Math Biol. 2021;82(1):1-25.
10. John W, Gould KG, Brown K. Richard Pfeiffer's typhoid vaccine and Almroth Wright's claim to priority. Vaccine. 2021;39(15):2074-2079. doi: 10.1016/J.VACCINE.2021.03.017.
11. Lema AB, Baisa B, Samuel K. Dynamics and control of typhoid fever in Sheno town, Ethiopia: A comprehensive nonlinear model for transmission analysis and effective intervention strategies. PLOS ONE. 2024. doi: 10.1371/journal.pone.0306544201.
12. Getachew M, Deressa A, Getachew Y. Mathematical modeling and optimal control of typhoid fever. J Biol Dyn. 2019;13(1):198-213.
13. Adeboye NO, Olaniyi SS, Okosun KO. Optimal control analysis of a mathematical model for typhoid fever. Int J Biomath. 2017;10(1):1750007.
14. Kraay AN, Yousafzai MT, Qureshi S, Gauld J, Qamar FN. Modeling the drivers of differential Typhoid Conjugate Vaccine (TCV) impact in Pakistan: force of infection and age-specific duration of protection. medRxiv. 2024:2024-08.
15. Cook J, Jeuland M, Whittington D. The contribution of direct and indirect benefits in the cost-effectiveness of vaccination. Vaccine. 2020;38(3):586-94.
16. Karunditu NG, Omolo MO, Otieno W. A nonlinear epidemic model for typhoid fever transmission. Int J Biomath. 2021;14(7):2150046.
17. Bhunu CP. Modeling the transmission dynamics of typhoid fever with a public health education campaign. Appl Math Model. 2016;40(4):2213-28.
18. Nyerere N, Mpeshe SC, Ainea N, Ayoade AA, Mgandu FA. Global sensitivity analysis and optimal control of typhoid fever transmission dynamics. Math Model Anal. 2024;29(1):141-60. Available from: https://journals.vilniustech.lt/index.php/MMA/article/view/17859.
19. Movaheedi Z. Analyzing the dynamic characteristics of a tuberculosis epidemic model using numerical methods. Afghanistan J Infect Dis. 2024. Available from: https://api.semanticscholar.org/CorpusID:270947479.
20. Mickens RE. Advances in the Applications of Nonstandard Finite Difference Schemes. Singapore: World Scientific; 2005.
21. Aljohani A, Shokri A, Mukalazi H. Analyzing the dynamic patterns of COVID-19 through nonstandard finite difference scheme. Sci Rep. 2024;14:8466. doi: 10.1038/s41598-024-57356-9.
22. Hoang MT, Ehrhardt M. A second-order nonstandard finite difference method for a

general Rosenzweig-MacArthur predator-prey model. J Comput Appl Math. 2024 Jul 1;444:115752.
23. Khan IU, Qasim M, El Koufi A, Ullah H. The stability analysis and transmission dynamics of the SIR model with nonlinear recovery and incidence rates. Math Probl Eng. 2022;2022(1):6962160.
24. Martcheva M. An introduction to mathematical epidemiology. New York: Springer US; 2016.
25. Wangari IM. Condition for global stability for a SEIR model incorporating exogenous reinfection and primary infection mechanisms. Comput Math Methods Med. 2020;2020:9435819. doi: 10.1155/2020/9435819.
26. Masood S, Bareera I, Shabbir J, Shokri A, Zabihullah Movaheedi. Estimating neutrosophic finite median employing robust measures of the auxiliary variable. Sci Rep. 2024 May 4;14(1).
27. Abboubakar H, Racke R. Mathematical modeling, forecasting, and optimal control of typhoid fever transmission dynamics. Chaos Solitons Fractals. 2021;149:111074.
28. Jan R, Boulaaras S, Alnegga M, Abdullah FA. Fractional-calculus analysis of the dynamics of typhoid fever with the effect of vaccination and carriers. Int J Numer Model. 2023 Oct 31;37(2).
29. Maji D, Ghosh A. Consequences of Parameters Mathematical Modelling of Two Interacting Viruses. In: Advances in bioinformatics and biomedical engineering. 2024. doi: 10.4018/979-8-3693-2655-8.ch009.
30. Carpio A, Pierret E. Mathematical Analysis of Infectious Diseases. Amsterdam: Elsevier BV; 2022.
31. Ibrahim B, Benoîte de S, Solym M, Manou-Abi M. Estimating parameters of continuous-time multi-chain hidden Markov models for infectious diseases. 2024. doi: 10.48550/arxiv.2403.18875.